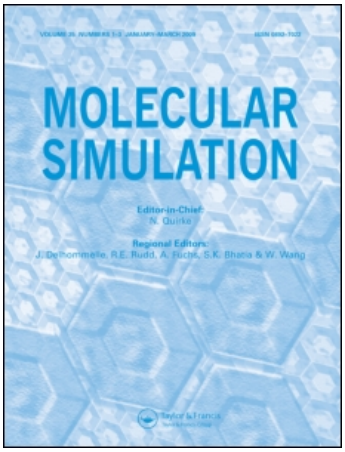

Molecular Simulation
Publication details, including instructions for authors and subscription information:
http://www.informaworld.com/smpp/title~content=t713644482

Molecular dynamics simulation of lipid bilayers with GROMOS96: Application of surface tension

I. Chandrasekhar[a]; D. Bakowies[a]; A. Glättli[a]; P. Hünenberger[a]; C. Pereira[a]; W. F. van Gunsteren[a]
[a] Laboratory of Physical Chemistry, Swiss Federal Institute of Technology Zürich, Zürich, Switzerland

To cite this Article Chandrasekhar, I. , Bakowies, D. , Glättli, A. , Hünenberger, P. , Pereira, C. and van Gunsteren, W. F.(2005) 'Molecular dynamics simulation of lipid bilayers with GROMOS96: Application of surface tension', Molecular Simulation, 31: 8, 543 — 548
To link to this Article: DOI: 10.1080/08927020500134243
URL: http://dx.doi.org/10.1080/08927020500134243

Molecular Simulation, Vol. 31, No. 8, July 2005, 543–548

Taylor & Francis
Taylor & Francis Group

Molecular dynamics simulation of lipid bilayers with GROMOS96: Application of surface tension

I. CHANDRASEKHAR*, D. BAKOWIES, A. GLÄTTLI, P. HÜNENBERGER, C. PEREIRA and W. F. VAN GUNSTEREN

Laboratory of Physical Chemistry, Swiss Federal Institute of Technology Zürich, ETH Hönggerberg, 8093 Zürich, Switzerland

(Received January 2005; in final form February 2005)

The GROMOS96 force fields 45A3 and 53A5, when applied to dipalmitoylphosphatidylcholine (DPPC) membranes, have a tendency to result in a reduced area per lipid in constant pressure simulations. The application of surface tension is effective in increasing the area per lipid, a measure of the phase of the membrane, but only if the area is already close to the experimental range. Therefore the surface tension cannot compensate for strong inadequacies in the force-field parameters. The behaviour of the 45A3 force field from long $NP_n\gamma T$ simulations of tens of nanoseconds is analysed over a range of different surface tensions. Comparisons are made with the corresponding NP_nAT simulations.

Keywords: Molecular dynamics simulation; GROMOS96; DPPC; Lipid bilayer membrane; Surface tension

1 Introduction

The inclusion of surface tension (γ) through the application of a constant negative lateral pressure (P_{lat}) during molecular dynamics (MD) simulation of lipid bilayer membranes has been the subject of much discussion [1–5]. On the one hand, it has been argued that a membrane that is not subject to osmotic stress is not under surface tension [1]. On the other hand, it has been pointed out that the microscopic and macroscopic implications of the change in the free energy of a bilayer with surface area are not the same [2,6]. The application of a negative lateral pressure during simulation is therefore suggested as a means of compensating for the finite size of the microscopic simulation cell that prevents long scale fluctuations in the simulated membrane [2]. It has been shown that the size of the simulation cell does indeed affect the long range fluctuations or undulations [7] and the surface tension inherent to the system [2]. Regardless of the physical implications, application of a negative lateral pressure during simulation results in an expanded membrane [2,7–10]. Most studies that demonstrated and discussed this were, however, based on simulations that were too short to allow for an adequate convergence of the relevant properties [7–12]. In this article we examine the effect of the application of a surface tension during simulation of hydrated lipid bilayer membranes using GROMOS96 over tens of nanoseconds.

The balance of interactions in hydrated lipid bilayers in the context of the GROMOS96 force-field and simulation parameters have been the subject of much of our efforts [13–18]. The improved alkane parameters of the united atom 45A3 force-field [13,14] were shown to be insufficient in maintaining the lipid bilayer in the liquid-crystalline phase during constant-pressure simulations above the phase transition temperature without an appropriate refinement of the charge distribution at the polar groups [13,17]. It should be noted that constant-pressure simulations refer to simulations with no surface tension applied. Association of water at the interfacial region, which is strongly affected by changes in the charge distribution, was shown to play a critical role in modulating the phase behaviour of the dipalmitoylphosphatidylcholine (DPPC) bilayer [18]. Significantly, the bilayer properties are mostly sensitive to the charge distribution at the relatively less exposed ester groups. The interactions between the polar groups and water are known to have an influence on the surface tension used during MD simulation [2,19]. The microscopic surface tension has been identified through a spatial and energetic-entropic decomposition of the different contributions to the free energy as being due to a balance between the attractive interactions between the polar groups and water

*Corresponding author. E-mail: indira@igc.phys.chem.ethz.ch

Molecular Simulation
ISSN 0892-7022 print/ISSN 1029-0435 online © 2005 Taylor & Francis Group Ltd
http://www.tandf.co.uk/journals
DOI: 10.1080/08927020500134243

and the tendency of the chains to expand [19]. This is in accord with the general understanding of lipid bilayer behaviour from theoretical considerations [20]. We evaluate the consequences of the application of surface tension in GROMOS96 bilayer simulations in the context of the interaction with water.

A series of $NP_n\gamma T$ simulations are analysed where, in addition to the number of particles N and the temperature T, the normal pressure P_n and the applied surface tension, γ, are kept fixed [21,22]. Different GROMOS96 force fields are employed. The simulations that range in length from 7 to 40 ns are subject to increasing values of the surface tension γ. The trajectories from NP_nAT simulations where the surface area, A, rather than γ is kept fixed are performed for comparison and validation.

2 Methods

All simulations are carried out using the simulation package GROMOS96 [23,24]. The initial model is a hydrated 128 DPPC bilayer that was previously equilibrated for 2.5 ns with the GROMOS96 force-field parameter set 45A3 [13,14] using the simulation conditions described in [17]. The 3655 water molecules in the system are represented using the SPC model [25]. In the present study, different parameter sets are considered. The charges are in all but one case taken from the charge set (C95) derived by Chiu and coworkers [10]. The names of the parameter sets reflect both the GROMOS96 force field and the charges used on the polar groups. Thus when the C95 charges are applied to all the polar groups in combination with the 45A3 force-field parameters, the parameter set is termed 45A3_C95. We also make use of the parameter set 53A5_C95sn2E where the charges for the sn2 ester moiety from the C95 charge set are applied to both ester groups. The modifications from the 53A5 to the 53A6 GROMOS96 force-field parameter set relate to the refinement of the charges of particular polar groups by fitting to the free energy of solvation of model compounds [26] and do not apply to the glycerolester-phosphatidylcholine head-group. Hence 53A5_C95sn2E and 53A6_C95sn2E are equivalent for glycerophospholipids. A triple range cut-off scheme is used to handle the non-bonded interactions, with short- and long- range cutoff radii of 0.8 and 1.4 nm and a pair list updated every 5 steps. Long-range electrostatic interactions are treated by application of a reaction-field correction based on solvent permittivity of 54.0 [27]. The simulations are run at 325 K and the temperature is maintained by coupling to a temperature bath with a coupling constant of 0.1 ps. The pressure tensor is coupled anisotropically to the pressure bath using a coupling constant of 0.5 ps [28]. In the case of the *NPT* simulations, the pressure bath is 1 bar in all directions and in the case of the $NP_n\gamma T$ simulations it is 1 bar in the normal direction and equal to the applied lateral pressure in the lateral directions. The surface tension, γ, is evaluated from the difference in the instantaneous values of the negative lateral pressure, P_{lat} and the normal pressure, P_n, modulated by the mean value of half the box size in the Z direction, L_z, as follows:

$$\gamma = L_z\{P_n + P_{lat}\} \quad (1)$$

where $P_{lat}(= 1/2[P_x + P_y])$ is given by half the sum of the instantaneous negative pressures P_x and P_y in the X and Y directions, respectively.

3 Results and discussion

3.1 Area per Lipid

One of the most frequently used measures of the phase of a lipid bilayer membrane is the area per lipid (A/l). The experimental evaluation of this parameter is dependent on the model and the approximations made to interpret the raw measurement as discussed by Nagle and Tristram-Nagle [29]. We compare the value calculated from our simulations against a range spanned by experimental numbers with reference to the ideal long chain value extrapolated from NMR experiments [30] and the theoretical target value suggested by an assessment of experimental methods [29]. In all cases the changes in the area per lipid result in consistent changes in the chain order parameters (data not shown). An increase in the area

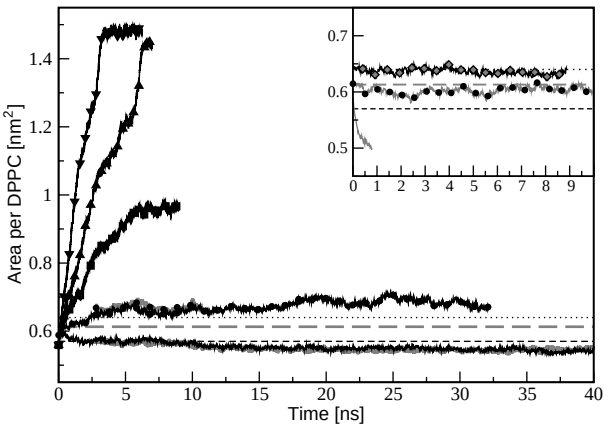

Figure 1. Area per lipid, A/l as a function of time for increasing negative lateral pressure, P_{lat}. The *NPT* simulations using the 45A3_C95 (thin black line) and 53A5_C95sn2E (thick grey line) force field parameter sets are shown for reference. The following symbols are imposed on the respective lines, to indicate the applied P_{lat} in the $NP_n\gamma T$ simulations: 100 bar (●), 200 bar (■), 250 bar (▲), 300 bar (▼). The inset where the axes (not labelled) are the same as in the main figure shows the A/l from the 45A3 *NPT* (thin grey line) and $NP_n\gamma T$ simulations with a P_{lat} of 170 bar (●). Also included in the inset is the result from the 45A3_C95 $NP_n\gamma T$ simulation with a P_{lat} of 78 bar (◆), which results in a A/l of 0.64 nm^2, the theoretical best estimate of the area per DPPC molecule in the liquid-crystalline phase [29]. Both the main figure and the inset indicate the lower limit of the range of experimental values [29] (horizontal black dashed line), the area per PC lipid from NMR experiments extrapolated to infinite chain length [30] (horizontal dashed thick grey line) and a theoretical best estimate of the area per DPPC molecule in the liquid-crystalline phase [29] (horizontal dotted black line).

accessible to each lipid results in a lower order parameter consistent with increased order.

In figure 1 is shown the time-evolution of A/l from the $NP_n\gamma T$ simulations with P_{lat} of increasing magnitude. Here, A/l is evaluated from the box dimensions, the assumption being that the bilayer remains intact through the simulation. As anticipated, A/l increases as the magnitude of P_{lat} increases. The simulations take approximately 5 ns or more to reach a plateau value, validating the statement that previously reported simulations studying the application of γ on membrane behaviour were short. In the $NP_n\gamma T$ 45A3_C95 simulation, a P_{lat} of 100 bar, which is equivalent, for this model, to a γ of approximately 32 mN m^{-1}, yields an A/l of 0.67 nm^2 (table 1). This value of γ is within the range identified by Pastor and co-workers as the correct surface tension to apply to a 2 × 36 DPPC membrane patch [8] although their simulations were at the time too short to distinguish between the different applied values. The A/l values for a P_{lat} of 200, 250 and 300 bar are 0.98 nm^2 at 9 ns, 1.43 nm^2 at 7 ns and 1.49 nm^2 at 6 ns, respectively (table 1). The fact that A/l as function of time reaches a plateau value does not imply a stable system. Panels a–d in figure 2 show snapshots from 45A3_C95 $NP_n\gamma T$ simulations with increasing values of γ. In all cases where P_{lat} is greater than 100 bar in magnitude, membrane disruption is observed. This is consistent with other studies evaluating [32] the sensitivity of the formation and stability of water pores to the applied γ during $NP_n\gamma T$ simulations of DPPC bilayers under stress using a variation of the GROMOS96 force-field parameters [23,24] combined with alkane van der Waals parameters due to Berger et al. [31] and the C95 charge set [10]. We observe lateral expansion of the simulation box and significant thinning of the membrane as the magnitude of P_{lat} increases. At a P_{lat} of 200 bar one begins to see evidence of the formation of a water pore in the middle of the membrane. On increasing P_{lat} to 250 bar the water pore dominates the box and the lipids aggregate. The dimension of the simulation box in the Z direction reduces to approximately one lipid length suggesting interdigitation. At a P_{lat} of 300 bar all semblance to a bilayer is lost and the water pore dominates the simulation box. In contrast, on application of a P_{lat} of 100 bar, the membrane retains its integrity even after 35 ns of simulation.

Results from the NPT simulations are also plotted in figure 1 for comparison. The 45A3_C95 and the 53A5_C95sn2E simulations yield a very similar A/l, which relaxes from approximately 0.57 to 0.54 nm^2 at the end of 40 ns. The 45A3 simulation has a A/l of 0.50 nm^2 at the end of 0.8 ns of simulation (the equilibrium value is probably still smaller). In this model the free energy of solvation of the ester groups is in better agreement with the experimental free energy of solvation of a series of model alkyl esters [18] but cannot induce adequate water association at the membrane interface (figure 4), resulting in a low A/l. A P_{lat} of 170 bar is required to yield a

Table 1. The area per lipid, A/l, box dimensions in the X, Y and Z directions, box volume, calculated surface tension γ from the NP_nAT and the stable $NP_n\gamma T$ simulations, the applied surface tension γ in the stable $NP_n\gamma T$ simulations and the negative lateral pressure, P_{lat}, used in the $NP_n\gamma T$ simulations.

	Model	*A/l* *(nm^2)*	*X* *(nm)*	*Y* *(nm)*	*Z* *(nm)*	*Volume* *(nm^3)*	$\gamma_{calculated}$ *(mN m^{-1})*	$\gamma_{applied}$ *(mN m^{-1})*	P_{lat} *(bar)*
Ensemble									
NPT	Parameter: **45A3**	0.50	5.60	5.68	8.43	268.3	–	–	
	Time: 0.8 ns	*0.02*	*0.11*	*0.13*	*0.30*	*0.6*			
$NP_n\gamma T$	Parameter: 45A3	0.60	6.03	6.42	7.03	271.7	–	–	170
	[a]Time: 10 ns	*0.01*	*0.05*	*0.10*	*0.06*	*0.5*			
NPT	Parameter: **45A3_C95**	0.57	5.89	6.22	7.30	267.3	–	–	–
	Time: 10 ns	*0.01*	*0.06*	*0.09*	*0.06*	*0.5*			
NP_nAT	Parameter: 45A3_C95	0.57	5.83	6.24	7.35	267.4	[b]5	–	–
	Time: 75 ns				*0.01*	*0.5*	*4*		
NP_nAT	Parameter: 45A3_C95	0.64	6.40	6.40	6.55	268.2	[b]25	–	–
	Time: 75 ns				*0.01*	*0.5*	*9*		
NP_nAT	Parameter: 45A3_C95	0.77	7.00	7.00	5.50	269.4	[b]42	–	–
	Time: 76 ns				*0.01*	*0.5*	*9*		
$NP\gamma_nT$	Parameter: 45A3_C95	0.64	6.39	6.37	6.59	268.3	25	25	78
	[a]Time: 10 ns	*0.01*	*0.08*	*0.06*	*0.05*	*0.5*	*1*		
$NP_n\gamma T$	Parameter: 45A3_C95	0.67	6.27	6.89	6.23	268.8	33	32	100
	Time: 32 ns	*0.02*	*0.16*	*0.17*	*0.14*	*0.5*	*3*		
$NP_n\gamma T$	Parameter: 45A3_C95	0.98	7.80	8.08	4.30	270.5	–	–	200
	Time: 9 ns	*0.11*							
$NP_n\gamma T$	Parameter: 45A3_C95	1.43	10.32	8.87	2.97	272.4	–	–	250
	Time: 7 ns	*0.24*							
$NP_n\gamma T$	Parameter: 45A3_C95	1.49	9.70	9.75	2.88	272.6	–	–	300
	Time: 6 ns	*0.28*							
NPT	Parameter: **53A5_C95sn2E**	0.55	5.97	5.89	7.63	268.4	–	–	–
	[a]Time: 40 ns	*0.01*	*0.05*	*0.10*	*0.11*	*0.5*			
$NP_n\gamma T$	Parameter: 53A5_C95sn2E	0.67	6.48	6.63	6.29	270.5	32	32	100
	[a]Time: 5 ns	*0.01*	*0.05*	*0.08*	*0.08*	*0.6*	*2*		

[a] The properties are averaged over the time period shown.
[b] Specified valves are averaged over the time period listed in column 2.
When not indicated, the properties are evaluated at the time point listed in column 2.

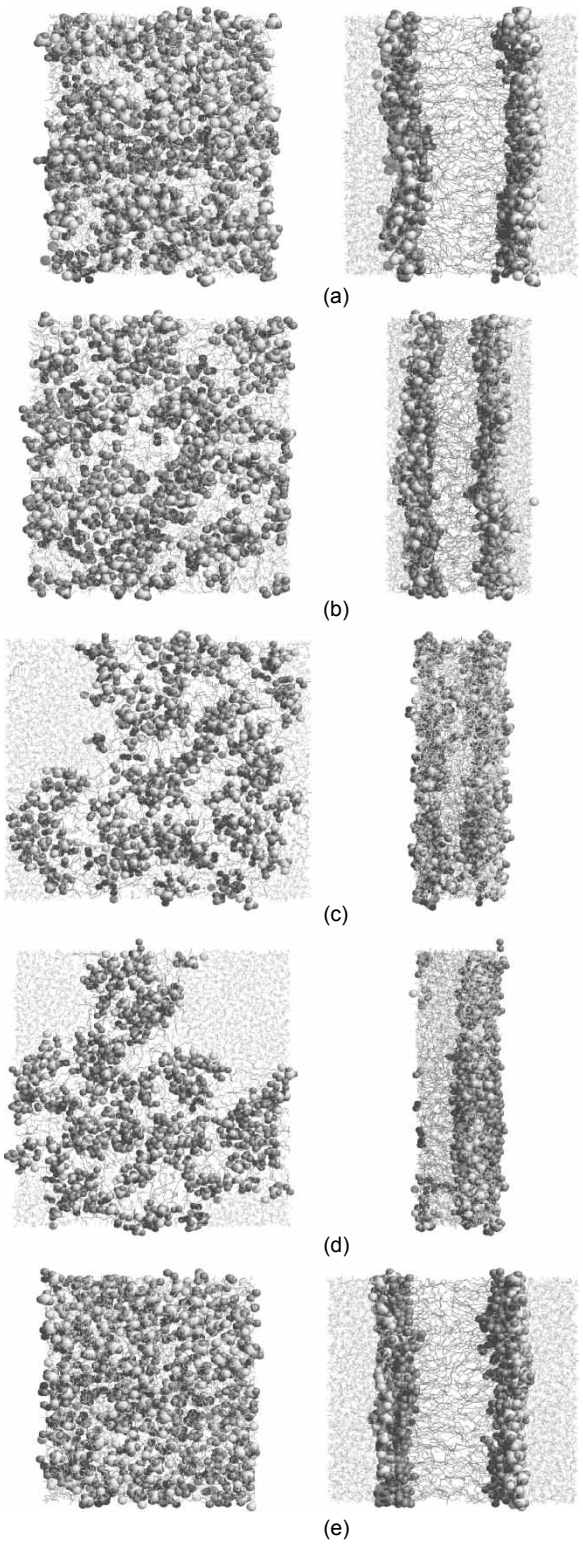

Figure 2. Snapshots of the hydrated DPPC bilayer, viewed down the z axis (left panel) and y axis (right panel) of the simulation box for the $NP_n\gamma T$ simulations at the specified times. (a) 45A3_C95: 100 bar at 32 ns (b) 45A3_C95: 200 bar at 12 ns (c) 45A3_C95: 250 bar at 6 ns (d) 45A3_C95: 300 bar at 6 ns and (e) 45A3: 170 bar at 10 ns. The alkane chains are shown as grey lines, the P and N atoms of the head-group as white spheres with radii proportional to the van der Waals radii of the respective atoms, the oxygen atoms as grey spheres whose radii are set proportional to 0.12 nm and the water molecules as light grey lines. The figures are not corrected for periodicity and are scaled by the same factor.

reasonable A/l. The membrane appears to be stable as suggested by the A/l after 10 ns of simulation (inset to figure 1). However, as seen in figure 2e, expansion induced by γ is in the alkane chain region but the polar interface is compact with reduced water penetration. Consequently the membrane begins to tear as evidenced by the water pore at the top right-hand, bottom left-hand corners of the simulation box. On visual inspection, the membrane surface is flatter than in the case of the model using 45A3_C95 that is simulated at a P_{lat} of 100 bar where there is some evidence of undulation. As the 45A3 simulation is discontinued on membrane disruption, we confine ourselves to a qualitative rather than a quantitative comparison.

3.2 Surface tension

Figure 3 shows the convergence of γ (cumulative average based on equation 1) with time in the following $NP_n\gamma T$ simulations: γ set at 78 and 100 bar using the 45A3_C95 set and at 100 bar using the parameter set 53A5_C95sn2e. Also shown are the γ values calculated from three NP_nAT simulations where A is kept fixed at values of 0.57, 0.64 and 0.77 nm^2. The box dimensions and γ values are listed in table 1. Also listed in table 1 for the stable $NP_n\gamma T$ simulations where the membrane retains its integrity are the applied lateral pressure translated into the corresponding γ and the γ calculated from the components of the pressure tensor (equation 1). Expectedly a larger value of A yields a larger value of γ in the NP_nAT simulations just as a larger value of γ results in a larger A/l in the $NP_n\gamma T$ simulations (figure 1). Since the volume of the simulation box remains approximately constant a larger γ leads to a thinning of the box or a reduction of the box size in the Z direction. The fluctuations of the box dimensions in the X and Y directions (time behaviour not shown) are correlated with the behaviour of A/l and the box dimension along z.

The NP_nAT simulation with $A = 0.64$ nm^2, the theoretical target value for DPPC [29], yields a γ of 25 mN m^{-1}. The positive value reflects the fact that simulations using the force-field parameter set 45A3_C95 in the absence of an included surface tension tend to a smaller A/l of 0.54 nm^2 (figure 1). In the case of a simulation box of 0.64 nm^2 per side the resulting surface tension is equivalent to a P_{lat} of 78 bar. As a consistency check, a $NP_n\gamma T$ simulation was performed with the same force field and an applied negative lateral pressure of 78 bar. As seen in the inset to figure 1, this simulation yields a perfectly consistent A/l of 0.64 nm^2.

3.3 Water at the interface

The importance of water association at the ester groups in determining bilayer properties from *NPT* simulations has been identified previously using the 45A3_C95 GROMOS96 force field [18]. In figure 4 the radial distribution function (rdf) of water at the pendant carbonyl oxygen atoms of the two ester groups from the $NP_n\gamma T$ simulations

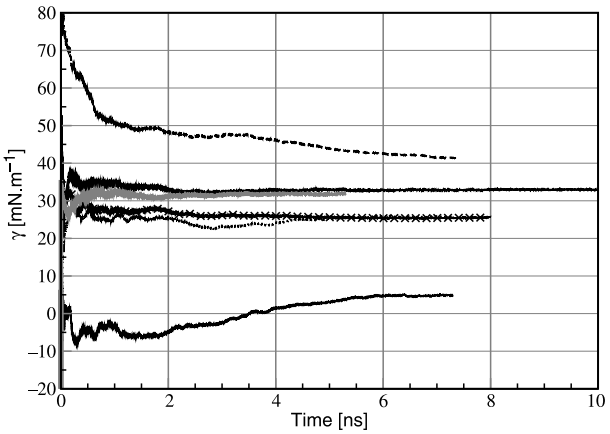

Figure 3. Cumulative average of the surface tension, γ, as a function of time for the three NP_nAT simulations using the 45A3_C95 force field. The area per lipid, A, is fixed at 0.57 nm^2, the A/l from the 45A3_C95 *NPT* simulation at the end of 10 ns (thin solid line), 0.64 nm^2, the theoretical target value suggested by Nagle and Tristram-Nagle [29] (dotted line) and 0.77 nm^2 (dashed line). Calculated γ values from the $NP_n\gamma T$ simulations using the 45A3_C95 parameters at 78 bar (solid line with crosses), 100 bar (thick solid line) and the 53A5_C95n2E parameters at 100 bar (thick grey line) are also shown. The applied γ in the 100 bar simulations is shown in alternate black and white squares for comparison.

is compared with those from the *NPT* simulations. In all cases except the 800 ps *NPT* simulation where the average is taken over 100 ps, the water distribution is averaged over 300 ps of simulation. The large first shell of water characteristic of the C95 sn2 ester charges [18] is evident. In the 45A3_C95 simulations it is observed only for the carbonyl atom of the sn2 chain, O22, as the C95 charge set has different values for the two ester groups. The number of waters is not affected by the decrease in A/l from 0.57 (2.6–2.9 ns) to 0.54 nm^2 (39.7–40.0 ns) in the *NPT* simulation. Application of a P_{lat} of 100 bar results in a small increase in the water aggregation, although it is not clear if this is statistically relevant. The first water shell around the less exposed pendant carbonyl atom of the sn1 chain, O12, is as expected, dependent on the charge set used. Water association at this group increases with increasing charge, i.e. upon going from 45A3 to 45A3_C95 to 53A5_C95sn2E. The expansion of the membrane for a P_{lat} of 100 bar has little effect on the rdf of the water at the O12 atom for all parameter sets.

4 Conclusions

Our intention in this article was to report basic results and fundamental analyses from long simulations, on the order of tens of nanoseconds, of hydrated DPPC bilayer membranes from different ensembles using different parameter sets developed in the context of the GROMOS96 force field. Results from *NPT*, NP_nAT and $NP_n\gamma T$ ensembles are discussed and compared. The calculated values of the surface tension in the $NP_n\gamma T$ simulations are equivalent to the corresponding applied negative lateral pressures. Furthermore, the surface tension evaluated from the NP_nAT simulations are consistent, showing that for a given force-field parameter set a chosen area per lipid yields a surface tension, which when applied during $NP_n\gamma T$ simulations results in an area per lipid which corresponds to the original chosen value. The significance of the interfacial water on regulating bilayer stability in

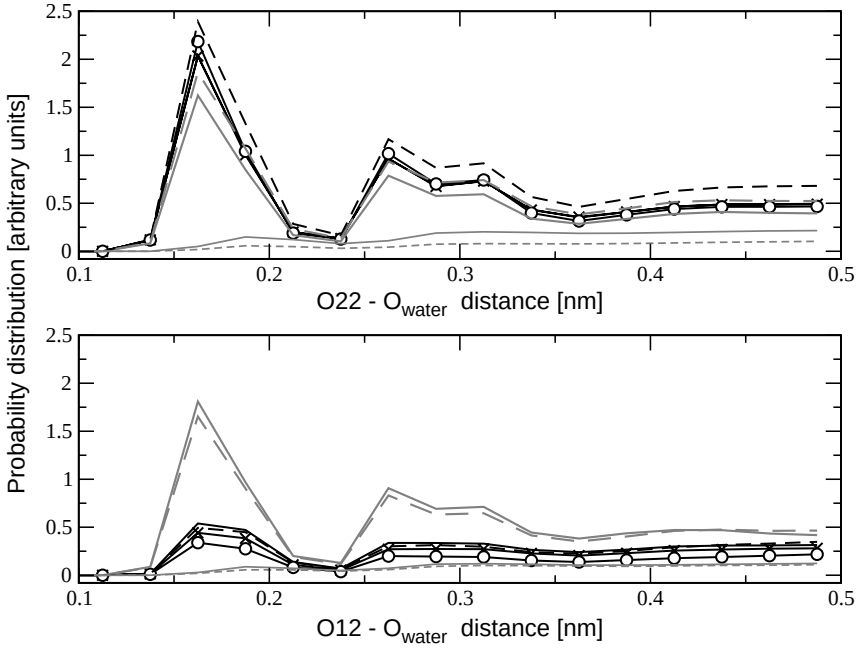

Figure 4. Radial distribution function, rdf, of water around the pendant carbonyl ester oxygen atom O12 of the sn1 chain (bottom panel) and O22 of the sn2 chain (top panel) averaged over 300 ps. The different simulations are: 45A3, *NPT* (thin grey line), 45A3, $NP_n\gamma T$ with a P_{lat} of 170 bar (thin dashed grey line), 45A3_C95, NPT 2.6–2.9 ns (black line), 45A3_C95 NPT 9.7–10.0 ns (black line with crosses), 45A3_C95, $NP_n\gamma T$ with a P_{lat} of 100 bar (dashed black line), 53A5_C95sn2E, *NPT* (thick grey line), 53A5_C95sn2E, $NP_n\gamma T$ with a P_{lat} of 100 bar (dashed thick grey line).

lipid bilayer membranes during MD simulation has been examined in the context of its dynamics and orientation [22,33,34]. It is clear from our results that the water behaviour is dominated by the charge distribution and that inclusion of surface tension during simulations has little effect on the interfacial water structure, even though it expands the bilayer and exposes the ester groups. We demonstrate further that although the surface tension serves as a means of increasing the surface area of the lipid bilayer, the bilayer remains intact only when the membrane is already expanded by water association at the interfacial region. The relaxation behaviour of different regions of the membrane in the different ensembles is currently under investigation and will be reported elsewhere.

Acknowledgements

The authors wish to acknowledge the National Center for Competence in Research (NCCR) in Structural Biology and the Swiss National Science Foundation for financial support.

References

[1] F. Jähnig. What is the surface tension of a lipid bilayer membrane? *Biophys. J.*, **71**, 1348 (1996).
[2] S.E. Feller, R.W. Pastor. On simulating lipid bilayers with applied surface tension: Periodic boundary conditions and undulations. *Biophys. J.*, **71**, 1281 (1996).
[3] B. Roux. Commentary: surface tension of biomembranes. *Biophys. J.*, **71**, 1346 (1996).
[4] D.J. Tobias, K. Tu, L. Klein. Atomic scale molecular dynamics simulations of lipid membranes. *Curr. Opin. Colloid Interface Sci.*, **2**, 115 (1997).
[5] D. Marsh. Renormalisation of the tension and area expansion modulus in fluid membranes. *Biophys. J.*, **73**, 865 (1997).
[6] S.H. White. Small phospholipid vesicles: Internal pressure, surface tension, and surface free energy. *Proc. Natl Acad. Sci. USA*, **77**, 4048 (1980).
[7] E. Lindahl, O. Edholm. Mesoscopic undulations and thickness fluctuations in lipid bilayers from molecular dynamics simulations. *Biophys. J.*, **79**, 426 (2000).
[8] S.E. Feller, R.W. Pastor. Constant surface tension simulations of lipid bilayer: The sensitivity of surface areas and compressibilities. *J. Chem. Phys.*, **111**, 1281 (1999).
[9] Y. Takaoka, M. Pasenkiewicz-Gierula, H. Miyagawa, K. Kitamura, Y. Tamura, A. Kusumi. Molecular dynamics generation of nonarbitrary membrane models reveals lipid orientational correlations. *Biophys. J.*, **79**, 3118 (2000).
[10] S.-W. Chiu, M. Clark, V. Balaji, S. Subramaniam, H.L. Scott, E. Jakobsson. Incorporation of surface tension into molecular dynamics simulation of an interface: A fluid phase lipid bilayer membrane. *Biophys. J.*, **69**, 1230 (1995).
[11] D.P. Tieleman, H.J.C. Berendsen. Molecular dynamics simulations of a fully hydrated dipalmitoylphosphatidylcholine bilayer with different macroscopic boundary condition and parameters. *J. Chem. Phys.*, **105**, 4871 (1996).
[12] D.P. Tieleman, S.J. Marrink, H.J.C. Berendsen. A computer perspective of membranes: molecular dynamics studies of lipid bilayer systems. *Biochim. Biophys. Acta*, **1331**, 235 (1997).
[13] L.D. Schuler. Molecular dynamics simulation of aggregates of lipids: Development of force field parameters and applications to membranes and micelles, Ph.D. Thesis 14009, ETH-Zürich, Zürich, Switzerland.
[14] L.D. Schuler, X. Daura, W.F. van Gunsteren. An improved GROMOS96 force field for aliphatic hydrocarbons in the condensed phase. *J. Comput. Chem.*, **22**, 1205 (2001).
[15] I. Chandrasekhar, W.F. van Gunsteren. Sensitivity of molecular dynamics simulations of lipids to the size of the ester carbon. *Curr. Sci.*, **81**, 1325 (2001).
[16] I. Chandrasekhar, W.F. van Gunsteren. A comparison of the potential energy parameters of aliphatic alkanes: Molecular dynamics simulations of triacylglycerols in the alpha phase. *Eur. Biophys. J.*, **31**, 89 (2002).
[17] I. Chandrasekhar, M. Kastenholz, R.D. Lins, C. Oostenbrink, L.D. Schuler, D.P. Tieleman, W.F. van Gunsteren. A consistent potential energy parameter set for lipids: dipalmitoylphosphatidylcholine as a benchmark of the GROMOS96 45A3 force field. *Eur. Biophys. J.*, **38**, 67 (2003).
[18] I. Chandrasekhar, C. Oostenbrink, F. van Gunsteren. Simulating the physiological phase of hydrated dipalmitoylphosphatidylcholine bilayers: The ester moiety. *Soft Mater.*, **2**, 27 (2004).
[19] E. Lindahl, O. Edholm. Spatial and energetic-entropic decomposition of surface tension in lipid bilayers from molecular dynamics simulations. *J. Chem. Phys.*, **113**, 3882 (2000).
[20] D. Marsh. Lateral pressure in membranes. *Biochim. Biophys. Acta*, **1286**, 183 (1996).
[21] Y. Zhang, S.E. Feller, B.R. Brooks, R.W. Pastor. Computer simulation of liquid/liquid interfaces. I. Theory and application to octane/water. *J. Chem. Phys.*, **103**, 10252 (1995).
[22] S.E. Feller, Y. Zhang, R.W. Pastor. Computer simulation of liquid/liquid interfaces. II. Surface tension-area dependence of a bilayer and monolayer. *J. Chem. Phys.*, **103**, 10267 (1995).
[23] W.F. van Gunsteren, S.R. Billeter, A.A. Eising, P.H. Hünenberger, P. Krüger, A.E. Mark, W.R.P. Scott, I.G. Tironi. *Biomolecular Simulation: The GROMOS96 Manual and User Guide*, vdf Hochschulverlag AG an der ETH Zürich and BIOMOS b v, Zürich, Groningen (1996).
[24] W.R.P. Scott, P.H. Hünenberger, I.G. Tironi, A.E. Mark, S.R. Billeter, J. Fennen, A.E. Torda, T. Huber, P. Krüger, W.F. van Gunsteren. The GROMOS biomolecular simulation program package. *J. Phys. Chem. A*, **102**, 3596 (1999).
[25] H.J.C. Berendsen, J.P.M. Postma, W.F. van Gunsteren, J. Hermans. Interaction models for water in relation to protein hydration. B. Pullman (Ed.), pp. 331–342, Reidel, Dordrecht (1981).
[26] C. Oostenbrink, A. Villa, A.E. Mark, W.F. van Gunsteren. A biomolecular force field based on the free enthalpy of hydration and solvation: the GROMOS force-field parameter sets 53A5 and 53A6. *J. Comput. Chem.*, **25**, 1656 (2004).
[27] I.G. Tironi, R. Sperb, P.E. Smith, W.F. van Gunsteren. A generalised reaction field method for molecular dynamics simulations. *J. Chem. Phys.*, **102**, 5451 (1995).
[28] H.J.C. Berendsen, J.P.M. Postma, W.F. van Gunsteren, A. DiNola, J.R. Haak. Molecular dynamics with coupling to an external bath. *J. Chem. Phys.*, **81**, 3684 (1984).
[29] J. Nagle, S. Tristram-Nagle. Structure of lipid bilayers. *Biochim. Biophys. Acta*, **1469**, 159 (2000).
[30] H.I. Petrache, S.W. Dodd, M.F. Brown. Area per lipid and acyl chain length distributions in fluid phosphatidylcholines determined by ^{2}H NMR spectroscopy. *Biophys. J.*, **79**, 3172 (2000).
[31] O. Berger, O. Edholm, F. Jähnig. Molecular dynamics simulations of a fluid bilayer of dipalmitoylphosphatidylcholine at full hydration, constant pressure and constant temperature. *Biophys. J.*, **72**, 2002 (1997).
[32] H. Leontiadou, A.E. Mark, S.J. Marrink. Molecular dynamics simulations of hydrophilic pores in lipid bilayers. *Biophys. J.*, **86**, 2156 (2004).
[33] S.J. Marrink, D.P. Tieleman, A.R. van Buuren, H.J.C. Berendsen. Membranes and water: An interesting relationship. *Faraday Discuss.*, **103**, 191 (1996).
[34] K. Aman, E. Lindahl, O. Edholm, P. Hakansson, O. Westlund. Structure and dynamics of interfacial water in an L_α phase lipid bilayer from molecular dynamics simulations. *Biophys. J.*, **84**, 102 (2003).